

PACS numbers: 42.55.Lt; 42.60.Lh
DOI: 10.1070/QE2001v031n08ABEH002029

Numerical simulation of electroionisation and electric-discharge gas flow CO lasers

Sh F Araslanov, R K Safiullin

***Abstract*. An effecient method is developed for numerical investigation of gas flow electric-discharge and electroionisation CO lasers. The model includes a set of vibrational kinetic equations, the equation for the electron energy distribution function, and radiative gas-dynamics equations. The proposed method is based on the splitting of the system of equations into several subsystems corresponding to different physical processes (splitting method). Populations of vibrational levels, the gains, the emission line intensities, the output power, and the efficiency of CO lasers are calculated and compared with the experimental data.**

Keywords: *CO laser, vibrational levels, gain, lasing spectrum*

1. Introduction

The development of effecient numerical methods for a correct description of the main processes occurring in CO lasers is associated with the quest for their optimal operational regimes. This problem has not lost its importance even today. The mathematical model proposed below for electric-discharge gas flow CO lasers contains a set of vibrational kinetics equations for the levels in CO and N_2 molecules, the equation for the electron energy distribution function (EEDF), gas-dynamic equations, and equations for the emission line intensities for a CO laser. This model is a continuation of the model [1] proposed by us earlier. Apart from the single-quantum transitions in CO molecules, this model can also be used for considering two- and multiquantum transitions. A programme has been developed for calculating the population of vibrational levels of CO and N_2 molecules, the gain and the emission line intensity, the output power, and the efficiency of CO lasers. The complex system of differential equations is solved by splitting it into several subsystems describing various physical processes (splitting method).

Sh F Araslanov N G Chebotarev Research Institute of Mathematics and Mechanics, Kazan State University, Universitetskaya ul. 17, 420008 Kazan, Russia; e-mail: ashamil@ksu.ru;
R K Safiullin Kazan State Academy of Architecture and Construction, ul. Zelenaya, 420043 Kazan, Russia; e-mail: sladkov@ksaba.ru

Received 19 February 2001
Kvantovaya Elektronika **31** (8) 697 – 703 (2001)
Translated by Ram Wadhwa

2. Vibrational kinetics equations

To describe the vibrational levels $E_n^{(1)}$ and $E_n^{(2)}$ of CO and N_2 molecules, we use the Morse anharmonic oscillator model:

$$E_n^{(j)} = E_1^{(j)} n - \Delta E^{(j)} n(n-1), \quad j = 1, 2, \quad n = 0, 1, \ldots,$$

$$E_1^{(1)} = 3084 \text{ K}, \ \Delta E^{(1)} = 18.7 \text{ K}, \ E_1^{(2)} = 3353 \text{ K}, \qquad (1)$$

$$\Delta E^{(2)} = 21.1 \text{ K}.$$

The value $n = 0$ corresponds to the zeroth (ground) vibrational level of the ground electronic state of CO and N_2 molecules. Calculations were carried out by taking into account up to 60 vibrational levels of CO and up to 50 vibrational levels of N_2.

In the CO – N_2 laser mixture, the following processes of vibrational – vibrational (VV) and vibrational – translational (VT) exchange were taken into account:

$$\text{CO}(n) + \text{CO}(m) \leftrightarrow \text{CO}(n-1) + \text{CO}(m+1), \qquad (2)$$

$$\text{N}_2(n) + \text{N}_2(m) \leftrightarrow \text{N}_2(n-1) + \text{N}_2(m+1), \qquad (3)$$

$$\text{CO}(n) + \text{N}_2(m) \leftrightarrow \text{CO}(n-1) + \text{N}_2(m+1), \qquad (4)$$

$$\text{CO}(n) + \text{CO} \leftrightarrow \text{CO}(n-1) + \text{CO}, \qquad (5)$$

$$\text{CO}(n) + \text{N}_2 \leftrightarrow \text{CO}(n-1) + \text{N}_2, \qquad (6)$$

$$\text{N}_2(n) + \text{CO} \leftrightarrow \text{N}_2(n-1) + \text{CO}, \qquad (7)$$

$$\text{N}_2(n) + \text{N}_2 \leftrightarrow \text{N}_2(n-1) + \text{N}_2. \qquad (8)$$

In addition, CO – He and CO – Ar laser mixtures were also considered.

It is convenient to introduce the normalised functions for the distribution of CO and N_2 molecules over vibrational levels:

$$f_n = \frac{N_n^{(1)}}{N^{(1)}}, \quad g_n = \frac{N_n^{(2)}}{N^{(2)}}, \qquad (9)$$

where $N^{(1)}$ and $N^{(2)}$ are the total densities of CO and N_2 molecules, respectively. In this case, the vibrational relaxation in the CO – N_2 mixture is described by the following

system of differential equations, taking into account the induced emission:

$$\frac{\mathrm{d}f_n}{\mathrm{d}t} = F_n + \left(\frac{\alpha_{n+1}I_{n+1}}{\Delta_n} - \frac{\alpha_n I_n}{\Delta_{n-1}}\right)\frac{T}{\xi_1 p} = F_n + \varphi_n\,, \qquad (10)$$

$$n = 0, 1, \ldots, v_1\,,$$

$$\frac{\mathrm{d}g_n}{\mathrm{d}t} = G_n\,, \quad n = 0, 1, \ldots, v_2\,. \qquad (11)$$

Here, F_n and G_n describe the VV- and VT-exchange processes (F_n also takes into account spontaneous emission from the excited vibrational levels of CO); T and p are the absolute temperature and pressure of the gas mixture, respectively; ξ_1 and ξ_2 are the molar fractions of CO and N_2; I_n and α_n are the intensity and the gain for the $n \to n-1$ emission line of the CO molecule, respectively; and $\Delta_n = E_{n+1}^{(1)} - E_n^{(1)}$. The expressions for F_n and G_n are presented in Refs [2–4].

Taking into account the overlap of the emission lines, the term φ_n in Eqn (10) can be replaced by the expression presented in Ref. [4].

3. Gas-dynamics equations

The one-dimensional vibrationally nonequilibrium flow of an inviscid CO–N_2 (CO–He, CO–Ar) gas mixture in a flat channel with a variable cross section is described by the equations

$$\rho u S = G = \mathrm{const}\,, \qquad (12)$$

$$\rho u \frac{\mathrm{d}u}{\mathrm{d}x} + \frac{\mathrm{d}p}{\mathrm{d}x} = 0\,, \qquad (13)$$

$$\rho u \frac{\mathrm{d}}{\mathrm{d}x}\left(c_p T + \frac{u^2}{2} + e_{\mathrm{vib}}\right) = \delta W - \sum_{v=1}^{v_1} \xi_1 \rho R E_v^{(1)} A_{v,v-1} f_v$$

$$- \sum_{v=1}^{v_1} \alpha_v I_v \equiv \psi\,, \qquad (14)$$

$$e_{\mathrm{vib}} = R\left(\xi_1 \sum_{v=1}^{v_1} E_v^{(1)} f_n + \xi_2 \sum_{v=1}^{v_2} E_v^{(2)} g_v\right), \qquad (15)$$

$$p = \rho R T\,. \qquad (16)$$

Here, x is the coordinate in the direction of the flow; ρ is the density of the gas and u is its velocity; $R = R_0/\mu$ is the gas constant; R_0 is the universal gas constant; μ is the molar weight of the mixture; $S = HL$ is the cross-sectional area of the channel; H is the height and L is the transverse size of the channel; G is the mass flow rate of the mixture through the channel; c_p is the translational-rotational specific heat of the gas at constant pressure ($c_p = 3.5R$ for the CO–N_2 mixture); $\delta = \delta_{\mathrm{el}} + \delta_{\mathrm{rot}} + \delta_{\mathrm{vib}}$ is the fraction of the specific power W transformed into translational, rotational and vibrational degrees of freedom of the molecules; and e_{vib} is the specific vibrational energy.

4. Equations for the emission line intensities

The output power of an electric-discharge CO laser with a Fabry–Perot cavity was calculated in the constant-gain approximation. The model assumes that, if the radiation is emitted at a certain vibrational–rotational transition $(n, j) \to (n-1, j+1)$, the following condition is satisfied at each cross section of the CO-laser cavity [4]:

$$\alpha'^{P}_{nj} = \alpha^{P}_{nj} + \sum_{k,m}\left(\alpha^{R}_{mk}\gamma^{PR}_{njmk} + \alpha^{P}_{mk}\gamma^{PP}_{njmk}\right)$$

$$= \alpha^* \equiv -\frac{\ln[(1-a)(1-a-\theta)]}{2L}, \qquad (17)$$

where α'^{P}_{nj} and α^{P}_{nj} are the gains for the P-transition $(n, j) \to (n-1, j+1)$ in CO taking the overlap of lines into account and neglecting it, respectively; α^* is the threshold gain; L is the separation between the mirrors, a is the absorption coefficient of the mirrors; and θ is the transmittance of the output mirror. It is assumed that for a given vibrational $n \to n-1$ transition, lasing occurs upon a change in the rotational quantum number $j_n \to j_n + 1$ corresponding to the maximum gain. Assuming an equilibrium distribution of the CO molecules over the rotational levels, the coefficient α^{P}_{nj} is calculated using the formula given in Ref. [5]. The line overlap factors γ^{PR}_{njmk} and γ^{PP}_{njmk} are described in Ref. [4] and are calculated using the line constants given in Refs [6–9].

The equations for the unknown intensities I_n are derived by differentiating (17) and equating the obtained expression to zero (taking into account the equations of vibrational kinetics).

If the line overlap is insignificant, we arrive at a three-diagonal system of algebraic equations [10]:

$$A_n I_{n+1} - B_n I_n + C_n I_{n-1} + D_n = 0, \quad n = l+1, \ldots, m\,. \qquad (18)$$

While deriving these equations, the terms containing $\mathrm{d}p/\mathrm{d}x$ and $\mathrm{d}T/\mathrm{d}x$ were omitted. In practical computations, the gains in formulas for calculating the coefficients A_n, B_n, C_n can be replaced by α^*. The system of equations (18) is solved by using the scalar sweep method. It is assumed that $I_l = 0$, $I_{m+1} = 0$. In the computational programme, the natural numbers l and m are determined in the course of computations.

Note that the emission line intensities can be calculated by a simpler and less time-consuming technique applicable for calculations with or without taking into account the overlap of lines. In this case, the following iterative formulas connecting the intensity and gain for a gas flow CO laser are used:

$$I_n^{(l)}(x + \Delta x) = I_n^{(l-1)}(x + \Delta x)\exp\left[\frac{\alpha'^{(l)}_{nj}(x + \Delta x)}{\alpha^*} - 1\right]. \qquad (19)$$

Here, l is the iteration number and Δx is the iteration step along the x axis. The value of the intensity at the preceding node can be taken as the initial approximation.

5. Boltzmann equation for the EEDF

To calculate the distribution of electrons over energy U, the expansion of the EEDF in Legendre polynomials was used. The Boltzmann equation for the spherically symmetric EEDF component was written in the form [11, 12]

$$\frac{1}{3}\left(\frac{E}{N}\right)^2 \frac{\mathrm{d}}{\mathrm{d}U}\left[U\frac{\mathrm{d}f}{\mathrm{d}U}\left(\sum_k \xi_k Q_k^{\mathrm{el}}\right)^{-1}\right] + \frac{kT}{e}\frac{\mathrm{d}}{\mathrm{d}U} \times$$

$$\times\left\{2U\frac{\mathrm{d}f}{\mathrm{d}U}\sum_k\xi_k\left[UQ_k^{\mathrm{el}}(U)\frac{m}{M_k}+3B_kQ_k^{\mathrm{rot}}(U)\right]\right\}$$

$$+\frac{\mathrm{d}}{\mathrm{d}U}\left\{2Uf(U)\sum_k\xi_k\left[UQ_k^{\mathrm{el}}(U)\frac{m}{M_k}+3B_kQ_k^{\mathrm{rot}}(U)\right]\right\}$$

$$+\sum_{kms}\xi_k\xi_{km}\left[(U+U_s)f(U+U_s)Q_s^{\mathrm{in}}(U+U_s)\right.$$

$$\left.-Uf(U)Q_s^{\mathrm{in}}(U)\right]+\sum_{kms}\xi_k\xi_{ks}\left(\frac{g_{km}}{g_{ks}}\right)\left[Uf(U-U_s)Q_s^{\mathrm{in}}(U)\right.$$

$$\left.-(U+U_s)f(U)Q_s^{\mathrm{in}}(U+U_s)\right]=0. \tag{20}$$

Here, e and m are the charge and mass of an electron; $\xi_k=N_k/N$; $N=\sum N_k$; $\xi_{km}=N_{km}/N$; N_{km} is the number of molecules of the kth species at the mth internal energy level; N is the total number of atoms and molecules per unit volume; M_k is the mass of the kth molecules; B_k, $Q_k^{\mathrm{el}}(U)$, $Q_k^{\mathrm{rot}}(U)$ are the rotational constant, transport cross section of the elastic scattering of electrons by the kth molecule and the excitation cross section for the rotational degrees of freedom of the kth molecule, respectively; U is the electron energy; U_s is the energy lost by an electron upon collision with a molecule of the kth species transferring the molecule from the mth to the sth internal energy level; Q_s^{in} is the cross section of such a process; and g_{km}, g_{ks} are the statistical weights of the levels m and s, respectively. The last two sums in Eqn (20) describe the inelastic and superelastic collisions of electrons with molecules, respectively.

The function $f(U)$ is subjected to the boundary condition $f(\infty)=0$ and the conventional normalisation condition

$$\int_0^\infty U^{1/2}f(U)\mathrm{d}U=1. \tag{21}$$

We solved equation (20) within a finite interval $(0, U_n)$. It was assumed that $f(U)=0$ for $U\geqslant U_n$. Equation (20) was approximated by a system of linear algebraic equations on the net U_i $(i=1\div n)$ with a variable step h_U. With an accuracy to a constant factor (which depends on the chosen interval of integration), the following partition of the integration domain was used: $h_U=0.01$ V, $0<U<0.5$ V, $h_U=0.05$ V, $0.5<U<5$ V, $h_U=0.20$ V, $5<U<15$ V. Such an arrangement of nodes in the net reflects the exponential variation in the EEDF, and was found to be quite useful in actual practice.

Disregarding the relaxation of the vibrational levels [i.e., considering Eqn (20) without the last sum], we can solve the system of equations by the method of elimination of unknown quantities [it is assumed that $f_{n-1}=1$, and f_{n-2}, f_{n-3}, etc. are determined successively up to $f_1\equiv f(0)$]. Then, the EEDF is normalised according to expression (21). Taking superelastic collisions into account, the system of equations is solved by the method of optimal elimination [13], which proves to be much more efficient than the conventional Gauss technique.

After finding the normalised EEDF, the rate constants of the processes involving electrons are calculated from the expression

$$K_{kms}=\left(\frac{2e}{m}\right)^{1/2}\int_0^\infty UQ_{kms}^{\mathrm{in}}(U)f(U)\mathrm{d}U. \tag{22}$$

Here, K_{kms} is the rate constant for excitation of the kth molecule from the m-level by an s-level electron ($m\rightarrow s$ transition). Fractions of the electric field energy corresponding to the inelastic (δ_{kms}), translational (δ_{el}), rotational (δ_{rot}), and vibrational degrees of freedom were also calculated, as well as the energy required for excitation of electronic levels and ionisation of atoms and molecules.

The rate constants for the inverse processes are calculated from the expression

$$K'_{kms}=\left(\frac{2e}{m}\right)^{1/2}\int_{U_{kms}}^\infty U\left(\frac{g_{ks}}{g_{km}}\right)$$

$$\times Q_{kms}(U)f(U-U_{kms})\mathrm{d}U. \tag{23}$$

Then, the fractions of energy corresponding to inelastic degrees of freedom of atoms and molecules (δ'_{kms}), translational degrees of freedom of atoms and molecules (δ'_{el}), and rotational degrees of freedom of molecules (δ'_{rot}) were calculated by using the well-known formulas.

Multiplying Eqn (20) by $U\mathrm{d}U$ and integrating from 0 to ∞, we arrive at the electron energy balance equation, which can be written in the form

$$\delta_{\mathrm{el}}+\delta_{\mathrm{rot}}+\sum_{kms}\delta_{kms}$$

$$-\left(1+\delta'_{\mathrm{el}}+\delta'_{\mathrm{rot}}+\sum_{kms}\delta'_{kms}\right)=0. \tag{24}$$

This relation is satisfied with a certain error Δ in computations. The relative error of our computations was written in the form:

$$\varepsilon=\left|\Delta\left(\delta_{\mathrm{el}}+\delta_{\mathrm{rot}}+\sum_{kms}\delta_{kms}\right)^{-1}\right|. \tag{25}$$

The cross sections for the processes of electron scattering by molecules presented in paper [11], which contains the results of many experimental and theoretical studies of cross sections, were used in our computations. In the programme used by us, the data base is stored as a one-dimensional array. It can be expanded by including other gas components, and can also be modified as more reliable data become available on the cross sections for the processes of electron scattering by atoms and molecules.

The integration domain was chosen in such a way that the relative variation in the EEDF within the domain was $10^{14}-10^{17}$. In the method of optimal elimination, the number of arithmetic operations is $\sim n^3$, where n is the number of nodes in the difference net. Calculations carried out for different mixtures show that for $n=191$, the relative computational error within the integration domain (0–15 V) is $\varepsilon\leqslant 0.02$, while for $n=300$, we have $\varepsilon\leqslant 0.01$. The time for calculating the EEDF on Pentium computers taking into account the relaxation is ~ 1 s for $n=191$. This makes it possible to recalculate the electron energy distribution and the integral characteristics of the EEDF at each step along the discharge chamber (or at each time step for electroionisation lasers).

6. Numerical method

The solution of the above system of equations simulating electric-discharge gas flow CO lasers, including the EEDF computation, is usually a complicated problem. The method proposed for calculating the vibrationally nonequilibrium flow of the CO–N_2 (CO–He, CO–Ar, etc.) laser mixture is in fact a splitting method which can be reduced to a successive separate solution of vibrational kinetics equations, gas-dynamics equations, and emission line intensity equations.

Thus, computations for an arbitrary cross section of the cavity can be reduced to the following 'global' iterative process: (1) determining the populations f_n, g_n of vibrational levels at the point x_{m+1} for known values of f_n, g_n at the point x_m and values of u, T, p, I_n at the points x_m, x_{m+1}; (2) determining the values of u, T, p at the point x_{m+1} for known f_n, g_n, I_n at the points x_m, x_{m+1}; and (3) computation of I_n at the point x_{m+1} for known f_n, g_n, u, T, p at the points x_m, x_{m+1}.

At the first stage of solution of the above problem, we applied the semi-implicit difference scheme to vibrational kinetics equations (10), (11) [14]

$$f_n^{m+1} - f_n^m = \Delta x\left[0.6\left(\frac{F_n}{u}\right)^{m+1} + 0.4\left(\frac{F_n}{u}\right)^m\right] + \varphi_n\,, \quad (26)$$

$$g_n^{m+1} - g_n^m = \Delta x\left[0.6\left(\frac{G_n}{u}\right)^{m+1} + 0.4\left(\frac{G_n}{u}\right)^m\right]. \quad (27)$$

Here,

$$F_n = A_n f_{n+1} + B_n f_n + C_n f_{n-1} + D_n\,, \quad (28)$$

$$G_n = A_n^* g_{n+1} + B_n^* g_n + C_n^* g_{n-1} + D_n^*, \quad (29)$$

where the coefficients A_n, B_n, C_n, A_n^*, B_n^*, C_n^* depend on f_0, f_1,...,f_{v_1}, g_0, g_1,..., g_{v_2}. Hence, for solving the system of nonlinear algebraic equations (26), (27), we use a sequence of two scalar sweeps with iterations.

The iterative method is constructed as follows. The initial values of population in the $m+1$-th layer are specified (these can be assumed to be equal to the values f_n, g_n at the preceding point x_m), and the coefficients A_n, B_n, C_n, A_n^*, B_n^*, C_n^* are calculated. To find the next approximation, we solved the systems of equations (26) and (27) by the sweep method. Then, the coefficients A_n, B_n, C_n, A_n^*, B_n^*, C_n^* were calculated again, and the process was repeated until the convergence of iterations was achieved.

We considered the single-quantum collision transitions and spontaneous VV transitions in CO molecules. Note that the importance of taking into account the multiquantum collision VV transitions in CO molecules for $n > 14$ was mentioned in Ref. [15]. Obviously, if we take into account the two-quantum VV transitions in the CO molecule, we should solve the five-diagonal systems of equations instead of three-diagonal systems of equations (26), (27). If three- and four-quantum VV transitions are taken into account, we should solve seven-diagonal and nine-diagonal systems of equations, respectively. However, we can confine the analysis to three-diagonal systems even for multiquantum VV transitions if the population of the levels separated from the one under study by distances $|\Delta n| \geqslant 2$ is taken from the preceding iteration.

At the second stage, the gas-dynamics equations (13), (14) are written in the form

$$\frac{\mathrm{d}h}{\mathrm{d}x} = \frac{\psi}{\rho u}, \quad h = c_p T + \frac{u^2}{2} + e_{\mathrm{vib}}\,, \quad (30)$$

$$\frac{\mathrm{d}q}{\mathrm{d}x} = p\,\frac{\mathrm{d}S}{\mathrm{d}x}\,, \quad q = Gu + pS\,. \quad (31)$$

This system of equations is solved by using the semi-implicit difference scheme [14]

$$h^{m+1} - h^m = \Delta x\left[0.6\left(\frac{\psi}{\rho u}\right)^{m+1} + 0.4\left(\frac{\psi}{\rho u}\right)^m\right], \quad (32)$$

$$q^{m+1} - q^m = \Delta x\left[0.6\left(p\,\frac{\mathrm{d}S}{\mathrm{d}x}\right)^{m+1} + 0.4\left(p\,\frac{\mathrm{d}S}{\mathrm{d}x}\right)^m\right]. \quad (33)$$

Taking into account the expression (30) for h, we obtain the following relation for p^{m+1} from (33):

$$p^{m+1} = \left[Gu^m + p^m S^m + 0.4\Delta x p^m\left(\frac{\mathrm{d}S}{\mathrm{d}x}\right)^m - Gu^{m+1}\right] \times \left[S^{m+1} - 0.6\Delta x\left(\frac{\mathrm{d}S}{\mathrm{d}x}\right)^{m+1}\right]^{-1}. \quad (34)$$

Equations (12) and (16) lead to the following expression for T^{m+1}:

$$T^{m+1} = \frac{p^{m+1}u^{m+1}S^{m+1}}{RG}. \quad (35)$$

Using expressions (34) and (35), we obtain from Eqns (30), (32)

$$c_p T^{m+1} + \frac{\left(u^{m+1}\right)^2}{2} + e_{\mathrm{vib}}^{m+1} - h^m = \frac{\Delta x\left(0.4\psi^m S^m + 0.6\psi^{m+1}S^{m+1}\right)}{G}. \quad (36)$$

Substituting relations (34) and (35) into this equation, we arrive at a quadratic equation in u^{m+1}, which can be written in the form

$$A\left[\left(u^{m+1}\right)^2 - \left(u^m\right)^2\right] + B\left(u^{m+1} - u^m\right) + C = 0\,, \quad (37)$$

where

$$A = 0.5 - \frac{c_p D}{R};$$

$$B = c_p D\left[Gu^m + p^m S^m + 0.4p^m\left(\frac{\mathrm{d}S}{\mathrm{d}x}\right)^m \Delta x\right](RG)^{-1};$$

$$D = S^{m+1}\left[S^{m+1} - 0.6\left(\frac{\mathrm{d}S}{\mathrm{d}x}\right)^{m+1}\Delta x\right]^{-1}; \quad (38)$$

$$C = A\left(u^m\right)^2 + Bu^m + e_{\mathrm{vib}}^{m+1} - h^m - \frac{\Delta x\left(0.4\psi^m S^m + 0.6\psi^{m+1}S^{m+1}\right)}{G}.$$

One of the roots of Eqn (37) corresponds to a subsonic gas flow, and the other to a supersonic flow.

Taking Eqn (37) into account, we determine the quantity u^{m+1} by using the following iterative procedure:

$$u_0^{m+1} = u^m,\ u_{k+1}^{m+1} = u^m - \frac{C}{A\left(u_k^{m+1} + u^m\right) + B}, \qquad (39)$$

$$k = 0, 1, 2, \ldots,$$

where k is the iteration number. In this case, the following convergence condition is employed:

$$\frac{\left|u_{k+1}^{m+1} - u_k^{m+1}\right|}{u_k^{m+1}} \leqslant \varepsilon. \qquad (40)$$

Computations show that the convergence for $\varepsilon \leqslant 10^{-3}$ is achieved after 1–3 iterations with a step $\Delta x = 0.01$ cm. Then, the values of p^{m+1} and T^{m+1} are obtained from expressions (34) and (35).

The third stage involving the computation of the line intensities was described in Section 4.

In the case of an electroionisation CO laser, the following system of equations is solved instead of Eqns (26) and (27):

$$f_n^{m+1} - f_n^m = \Delta t\left[0.6(F_n)^{m+1} + 0.4(F_n)^m\right] + \varphi_n, \qquad (41)$$

$$g_n^{m+1} - g_n^m = \Delta t\left[0.6(G_n)^{m+1} + 0.4(G_n)^m\right], \qquad (42)$$

while instead of Eqn (19), we solve the equation

$$I_n^{(l)}(t + \Delta t) = I_n^{(l-1)}(t + \Delta t)\exp\left[\frac{\alpha_{nj}^{\prime(l)}(t + \Delta t)}{\alpha^*} - 1\right], \qquad (43)$$

where Δt is the iteration step.

Our calculations show that the gas-dynamic parameters u, T, p at the point x_{m+1} can be calculated just after iterative calculations of f_n, g_n, I_n at this point. In other words, the second stage can be excluded from the 'global' iteration.

7. Results and discussion

Fig. 1 shows the schematic diagram of an electric-discharge gas flow CO laser used in our computations. The gas flow is directed along the x axis. The specific pump power W as a function of the coordinate x is specified on the interval $0 \leqslant x \leqslant x_H$.

Fig. 2 shows the theoretical dependences of the efficiency on the specific input power W for a gas flow laser with the $CO : N_2 = 1 : 9$ mixture composition, obtained under different conditions. One can see that a consideration of the superelastic collisions predicts an increase, saturation and a subsequent slight decrease in the laser efficiency with increasing the discharge power. This can be attributed to a redistribution of the vibrational excitation energy from CO molecules to N_2 molecules caused by superelastic collisions of electrons with these molecules. This mechanism was proposed in paper [16] devoted to pulsed CO lasers.

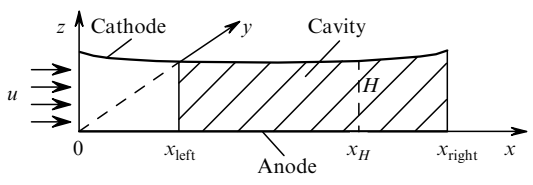

Figure 1. Schematic diagram of an electric-discharge gas flow CO laser: $0 \leqslant x \leqslant x_H$ is the region of electric discharge between a cathode and an anode, and $x_{left} \leqslant x \leqslant x_{right}$ is the region of the Fabry–Perot cavity arranged parallel to the y axis.

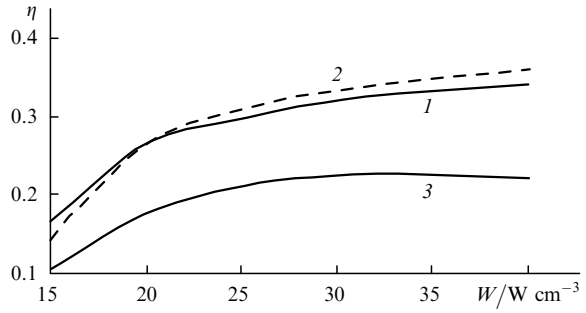

Figure 2. Theoretical dependences of the efficiency η of a gas flow CO laser on the deposited specific power W for a constant gain (curve 1), constant intensity (curve *2*) and constant gain taking into account the superelastic collisions (curve *3*) for $E/N = 2 \times 10^{17}$ V cm^2, pressure at the inlet to the discharge-cavity chamber $p = 10$ kPa, $T = 90$ K, $u = 70$ m s^{-1}, discharge chamber length $x_H = 9$ cm and cavity parameters $x_{left} = 4$ cm, $x_{right} = 10$ cm, $a = 0.01$, $\theta = 0.4$, $L = 40$ cm, and $H = 1$ cm.

Fig. 3 shows the theoretical emission spectrum of a CO laser for the $n \to n - 1$ transitions. The distribution of the gains $\alpha_{6j_6}^P$ and $\alpha_{8j_8}^P$ along the x axis, calculated by the constant intensity method, is shown in Fig. 4. The maxima of the gain are achieved just in front of the cavity. This is followed by a rapid decrease in the inverse population, and both values of the gain are slightly higher than the threshold value $\alpha^* \approx 0.67$ m^{-1} in the interval $4.5 < x < 9$ cm. When the pumping is switched off ($x = 9$ cm), the value of the coefficients $\alpha_{6j_6}^P$ and $\alpha_{8j_8}^P$ drops to 0.35 m^{-1}.

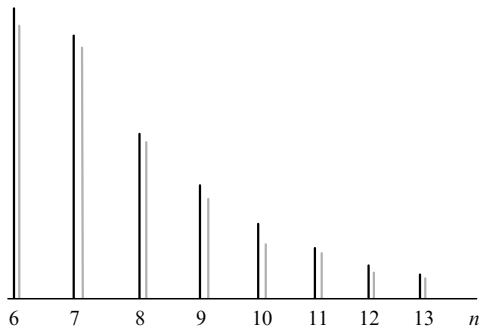

Figure 3. CO laser emission spectra calculated by the constant intensity method (dark lines) and constant gain method (grey lines).

Consider now the results of computations for pulsed electroionisation CO lasers. Fig. 5 shows the dependences of the specific laser energy Q_{rad} on the specific discharge energy $Q = en_e v_e E\tau$, where n_e is the concentration of electrons; v_e is their drift velocity; E is the applied electric field strength; and τ is the pump pulse duration. Curve *1* corresponds to the theoretical values obtained upon varying E/N in the interval $2.45 - 4.0 \times 10^{-17}$ V cm^2, while curve *2* is con-

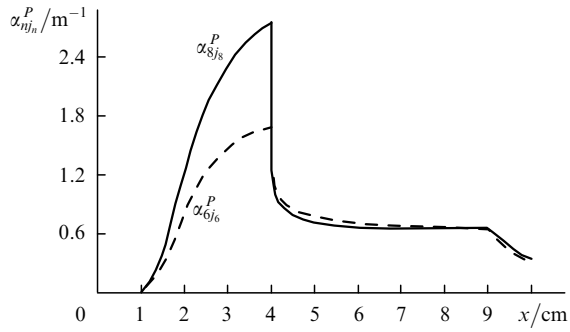

Figure 4. Spatial distribution of the gains $\alpha^P_{8j_8}$ and $\alpha^P_{6j_6}$ along the discharge cavity chamber.

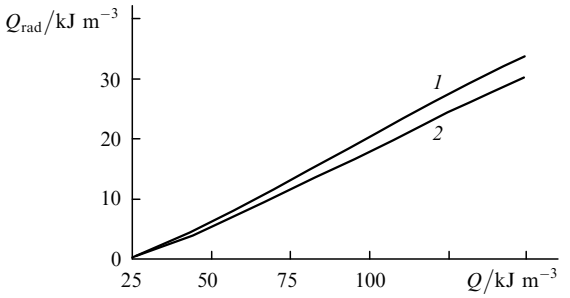

Figure 5. Theoretical (*1*) and experimental (*2*) dependences of the specific radiation energy Q_{rad} on the deposited specific energy Q for a pulse CO laser. The mixture composition CO : N_2 = 1 : 6, initial gas temperature $T = 100$ K, and pressure $p = 18.3$ kPa, $\tau = 100$ μs, $\alpha^* = 0.4\ \mathrm{m}^{-1}$.

structed from the experimental data obtained in Ref. [17]. The parameters E/N for which the theoretical values of Q_{rad} coincide with the experimental values proved to be smaller than the parameters obtained in the experiment.

Fig. 6 shows the output energy distribution for different transitions and the energy deposition for $\tau = 100$ μs. The grey lines correspond to calculations for the values of the parameters E/N selected to attain a coincidence of the theoretical and experimental values of Q_{rad}. Calculations made for experimentally determined values of E/N [17] give excessive values of the efficiency and emission spectra shifted to the blue. The results do not vary significantly if the line overlap for the pressures mentioned here is taken into account. A better agreement between the theoretical and experimental results could perhaps be attained by taking the isotopic composition of CO into account.

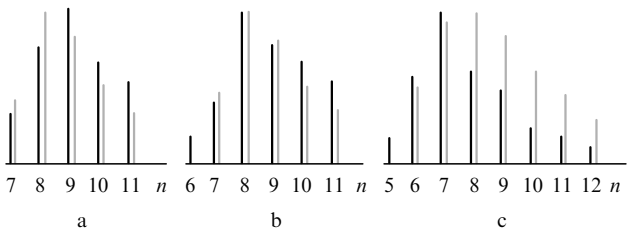

Figure 6. Distribution of the output radiation energy over vibrational levels for $\tau = 100$ μs, $Q = 50$ (a), 60 (b) and 120 J litre^{-1} (c). The dark lines correspond to the experiment [17], and the grey ones to the theoretical results obtained for $E/N = 2.46 \times 10^{-17}$ (a), 2.7×10^{-17} (b) and 3.8×10^{-17} V cm^2 (c).

The output power distributions over vibration levels calculated for a pulsed CO laser are presented in Fig. 7 for different values of E/N together with the experimental results [18, 19]. One can see that the energy contribution corresponds to the reduced electric field strength $E/N = 8.7 \times 10^{-17}$ V cm^2 at the initial instant of time. Because the field strength did not change by more than 30 % in the discharge gap in the experiments, the value of E/N was assumed to be constant in calculations. Note that the results of calculations almost do not change and the agreement between the theory and experiment does not improve if the line overlap is taken into account. Such an improvement is achieved by artificially reducing the value of E/N from 8.7×10^{-17} to 3.57×10^{-17} V cm^2.

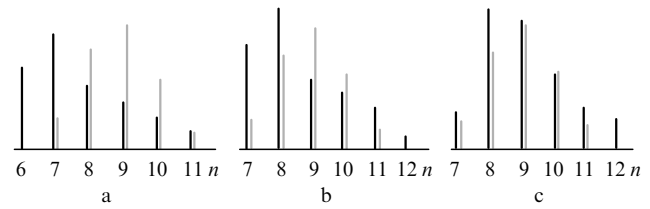

Figure 7. Energy distribution of the output radiation over vibrational levels for an initial pressure $p = 18.6$ kPa, $T = 100$ K, $W = 2$ kW cm^{-3}, $\tau = 100$ μs, $\alpha^* = 0.4\ \mathrm{m}^{-1}$. The dark lines correspond to calculations taking into account the overlap of lines for $E/N = 8.7 \times 10^{-17}$ (a), 4.5×10^{-17} (b) and 3.5×10^{-17} V cm^2 (c). The grey lines correspond to the experiment [18, 19] for $E/N = 8.7 \times 10^{-17}$ V cm^2.

Fig. 8 shows dependences similar to those shown in Fig. 7, but for different values of the initial parameters. One can see that even for a considerable increase in pressure, which increases the emission line overlap, the emission spectrum is displaced to the red by no more than $\Delta n = 1$. An analysis of the obtained results leads to the conclusion that the line overlap causes the red shift of the emission spectrum and a decrease in the laser efficiency.

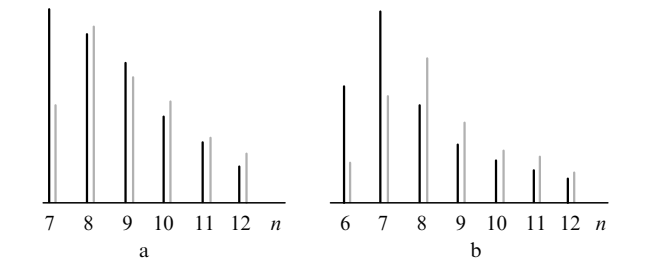

Figure 8. Energy distribution of the output radiation over vibrational levels calculated taking into account the line overlap (grey lines) and disregarding the line overlap (dark lines) for an initial pressure $p = 53.2$ kPa, $T = 100$ K, $W = 16.3$ kW cm^{-3}, $\tau = 35$ μs, $\alpha^* = 0.4\ \mathrm{m}^{-1}$, $E/N = 4.5 \times 10^{-17}$ (a) and $E/N = 8.7 \times 10^{-17}$ V cm^2 (b).

8. Conclusions

We have proposed an efficient method for calculating the electric-discharge gas flow lasers and pulsed electroionisation lasers. The mathematical model of the electric-discharge gas flow CO laser contains 110 vibrational kinetics equations for CO and N_2 molecules, radiation gas-dynamics equations, as well as the equation for the electron energy distribution function. Our calculations showed that

it is sufficient to take into account 20 vibrational levels of nitrogen and 40 vibrational levels of carbon monoxide, because the population of higher levels is negligibly small. The method proposed here is in fact a splitting method and allows one to solve a system of vibrational kinetics equations, gas-dynamic equations, and equations for the emission line intensities in the cavity separately. The programme developed in this work can be used for calculation of the population of the vibrational levels of CO and N_2 molecules, the gains for vibrational–rotational transitions in CO, the emission line intensity in the CO laser, as well as its output power and efficiency. The discrepancy between the theoretical and experimental results can be explained by the fact that the fraction of the electric power contribution to the translational and rotational degrees of freedom of molecules calculated from the EEDF is smaller than the experimentally measured value. The model can also be improved by taking into account the two-quantum and multiquantum VV transitions in a CO molecule.

References

1. Araslanov Sh F, Safiullin R K, in *Mater. Dokl. II Mezhdunar. Simp. Po Energetike, Okruzhayushchei Srede i Ekonomike* (Proc. II Intern. Symp. On Energetics, Environments and Economics) (Kazan', 1998) Vol. II, p. 80
2. Gordiets B F, Osipov A I, Shelepin L A *Kineticheskie Protsessy v Gazakh i Molekulyarnye Lazery* (Kinetic Processes in Gases and Molecular Lasers) (Moscow: Nauka, 1980)
3. Danilychev V A, Kerimov O M, Kovsh I B *Molekulyarnye Gazovye Lazery Vysokogo Davleniya* (Molecular High-Pressure Gas Lasers) (Itogi Nauki i Tekhniki. Ser. Radiotekhnika. Moscow, 1977) Vol. 12
4. Bulavin R E, Buchanov V V, Molodykh E I *Kvantovaya Elektron.* **11** 688 (1984) [*Sov. J. Quantum Electron.* **14** 467 (1984)]
5. Didyukov A I, Kirko V Yu, Kulagin Yu A, Shelepin L A *Trudy FIAN* **144** 107 (1984)
6. Konev Yu B, Kochetov I V, Pevgov V G, Sharkov V F *Preprint IAE* No. 2821 (Moscow, 1977)
7. Huber K-P, Herzberg G *Molecular Spectra and Molecular Structure* (New York: Van Nostrand 1979)
8. Antz A W, Maillard J-P, Roth B W, Narahari Rao K *Mol. Spectrosc.* **57** 155 (1975)
9. Losev S A, Makarov V N , in *Teoreticheskie issledovaniya protsessov v gazodinamicheskikh lazerakh* (Theoretical Studies of Processes in Gasdynamic Lasers) (Moscow, 1979) p. 87
10. Konev Yu B, Kochetov I V, Pevgov V G *Zh. Tekh. Fiz.* **49** 1266 (1979)
11. Araslanov Sh F *Raschet funktsii raspredeleniya elektronov po tnergiyam v slaboionizovannoi plazme razryada v smesi gazov CO_2, N_2, CO, O_2, H_2, He* (Computation of Electron Energy Distribution Function in Weakly Ionised Discharge Plasma in a Mixture of Gases CO_2, N_2, CO, O_2, H_2, He) (Kazan': Chebotarev Research Institute of Mathematics and Mechanics, Kazan State University. Manuscript deposited in VINITI, No. 2187-B87, 1987)
12. Araslanov Sh F, Safioulline R K *Izv. Vyssh. Uchebn. Zaved. Ser. Probl. Energ.* (8) 61 (1999)
13. Krylov V I, Bobkov V V, Monastyrnyi P I *Vychislitel'nye metody* (Computational Techniques) (Moscow: Nauka, 1976) Vol. 1
14. Losev S A *Gazodinamicheskie lazery* (Gas-dynamic Lasers) (Moscow: Nauka, 1977)
15. Ionin A A, Klimachev Yu M, Konev Yu B, et al. *Kvantovaya Elektron.* **30** 573 (2000) [*Quantum Electron.* **30** 573 (2000)]
16. Islamov R Sh, Konev Yu B, Kochetov I V, Kurnosov A K *Kvantovaya Elektron.* **11** 210 (1984) [*Sov. J. Quantum Electron.* **14** 147 (1984)]
17. Basov N G, Danilychev V A, Ionin A A, et al. *Kvantovaya Elektron.* **6** 1215 (1979) [*Sov. J. Quantum Electron.* **9** 716 (1979)]
18. Basov N G, Danilychev V A, Ionin A A, Kovsh I B *Trudy FIAN* **116** 54 (1979)
19. Basov N G, Danilychev V A, Ionin A A, et al. *Kvantovaya Elektron.* **6** 1208 (1979) [*Sov. J. Quantum Electron.* **9** 711 (1979)]